Preprints, 4th IFAC Conference on
Advances in Proportional-Integral-Derivative Control
Almería, Spain | June 12-14, 2024

Robust Fractional Order PID Controller Coupled with a Nonlinear Filtered Smith Predictor for Solar Collector Fields ⋆

Igor M. L. Pataro * **Juan D. Gil** * **José D. Álvarez** *
José L. Guzmán * **Manuel Berenguel** *

* *University of Almería, CIESOL, ceiA3, Department of Informatics, 04120 Almería, Spain (e-mail: ilp428@inlumine.ual.es)*

Abstract: This work introduces a Fractional Order PID (FOPID) controller associated with a nonlinear Filtered Smith Predictor (FSP) to control a Solar Collector Field (SCF) system. The combined approach enhances the control performance by decoupling model uncertainties. First, the FOPID addresses linear model uncertainties through optimal robust design across the operational conditions, while the FSP compensator adeptly manages the system's varying time delays. Rigorous tuning in the frequency domain considering closed-loop, robustness, and disturbance rejection performances is developed using a bi-level optimization approach to obtain the FOPID control parameters. Experimental results of the FOPID + nonlinear FSP demonstrate low rise time for reference tracking and robust stability across several operating conditions, even in the face of high-frequency disturbances in the solar irradiance due to passing clouds. Moreover, the nonlinear FSP effectively handles variations in time delays undergone by the water flow variation during the experiment. The achieved outcomes of the overall control structure, comprising the FOPID + FSP, demonstrate a promising approach for SCF system control, obtaining robust behavior in the presence of model uncertainties and disturbances while offering satisfactory reference tracking capabilities across an extensive range of plant operations.

Keywords: Fractional Order PID controller, Fractional PID tuning, Solar collector fields, Solar energy

1. INTRODUCTION

In control engineering, a fractional order PID ($PI^{\lambda}D^{\mu}$ or FOPID) controller is an extension of the classical PID controller, which incorporates integral and derivative actions defined for arbitrary (real) order indices. Since its introduction in (Podlubny, 1994), FOPID controllers have been studied for distinct designs and tuning methods to achieve superior performance compared to classical PID design (Shah and Agashe, 2016). The outcome has been a remarkable enhancement in loop shaping and a more robust control loop behavior, often proving unattainable for the classical PID controller.

The FOPID controller attributes hold significant promise in complex system control. Specifically, controlling Solar Collector Field (SCF) systems within solar plants presents an intriguing challenge. The discontinuous nature of solar irradiance and the nonlinear dynamics and variable time delays inherent to SCFs challenge classical PID control schemes (Camacho et al., 2012). In this context, adopting a FOPID controller emerges as a crucial means to enhance the performance of solar plants. Review works of FOPID controllers have showcased their capability to outperform conventional PID controllers in various critical scenarios (Shah and Agashe, 2016). These include demonstrating superior iso-damping characteristics, effectively handling systems with long delays, ensuring robust stability in challenging situations, and delivering more refined control for nonlinear and non-minimum phase systems. Therefore, the study of FOPID in SCFs is attempting since the control features address all the mentioned system complexities, enhancing solar plant control efficiency.

Several works have investigated FOPID for renewable systems (Alilou et al., 2023; Singh et al., 2020). However, few studies have delved into this approach concerning SCFs. First, Elmetennani et al. (2017) introduced a FOPID control strategy for parabolic troughs grounded in frequency domain performance analysis through simulation experiments. The approach involves optimizing FOPID parameters for robustness, reference tracking, and disturbance rejection performances in a closed-loop system. Similarly, Meng et al. (2020) followed an analogous methodology when studying FOPID in parabolic distributed solar collectors, applying statistical tests to evaluate various optimization algorithms. Noteworthy contributions by Beschi et al. (2016) involve implementing a FOPID controller in a solar furnace thermal facility, employing a frequency domain-based design for a gain-scheduling FOPID controller, and applying a similar tuning strategy to the earlier works.

⋆ This work has been funded by the National R+D+i Plan Projects PID2020-112709RB-C21, PID2021-126889OB-I00 of the Spanish Ministry of Science and Innovation and EIE funds. Igor M. L. Pataro acknowledges the financial support of the National Council for Scientific and Technological Development (CNPq, Brazil) under grant 201143/2019-4.

Based on the previous review, this work proposes a FOPID to assess robustness, reference tracking, and disturbance rejection performances in SCF systems. The control tuning is formulated over a bi-level optimization solution using global and local optimization algorithms to tune the FOPID parameters. The control tuning considers the uncertainties of the linearized model from the nonlinear lumped-parameters equation of the system dynamic model. The obtained controller is applied in the real-world system in the Solar Energy Research Center (CIESOL) at the University of Almería, southern Spain. Moreover, the FOPID is implemented considering an advanced dead-time compensator structure based on a nonlinear Filtered Smith Predictor (FSP) (Normey-Rico and Camacho, 2007) to assess the time-varying delay presented in the system.

The results presented here differ from the previous works in Elmetennani et al. (2017); Meng et al. (2020) mainly in two aspects. First, the control structure considers the system delays, a crucial aspect of the SCF process control. Secondly, a nonlinear FSP is applied in addition to a single FOPID controller to deal with the variation of system delays. This approach improves the control structure by allowing the FOPID to deal with linear model uncertainties through a robust design considering the complete operating range. At the same time, the FSP compensator handles the varying time delay, increasing the overall robustness and closed-loop performance of the control framework. After a comprehensive analysis of the control performance, the FOPID is implemented in an actual facility, proving the effectiveness of the presented strategy.

This work is organized as follows: Section 2 details the CIESOL SCF system model. Section 3 presents the details for tuning the FOPID control parameters. In Section 4, the results of the implementation of the FOPID in the CIESOL facility are presented. Finally, Section 5 discusses the achieved results.

2. CIESOL SOLAR COLLECTOR FIELD MODELING

The CIESOL plant employs the flat-plate SCF to produce hot water, serving as a thermal energy source for a heat exchanger or an absorption machine based on seasonal demand. In this work, a lumped-parameters model is used to describe the outlet temperature dynamic in the form of the following equation

$$\begin{aligned}\frac{dT_{sc,o}(t)}{dt} &= \frac{\beta}{\rho \cdot C_p \cdot A_{sc}} \cdot I(t) \\ &- \frac{H}{\rho \cdot C_p \cdot A_{sc} \cdot L} \cdot \left(\frac{T_{sc,o}(t) + T_{sc,in}(t - t_{d_{T_{in}}})}{2} - T_a(t) \right) \\ &- \frac{q(t - t_{d_q})}{A_{sc} \cdot c_f} \cdot \frac{T_{sc,o}(t) - T_{sc,in}(t - t_{d_{T_{in}}})}{L},\end{aligned} \tag{1}$$

in which $T_{sc,o}(t)$ [°C] is the outlet water temperature, $T_{sc,in}(t)$ [°C] is the inlet water temperature, $I(t)$ [W/m^2] is the solar irradiance, and $T_a(t)$ [°C] is the ambient temperature. In this system, the manipulated variable is the water flow $q(t)$ [m^3/h], and the controlled variable is $T_{sc,o}(t)$. The time delay $t_{d_{T_{in}}}$ is related to the inlet temperature, and t_{d_q} is associated with the water flow rate. As defined in Normey-Rico et al. (1998), the time delay depends on the water flow rate, causing a varying time-delay behavior, that is, $d_q(q(t))$. In Eq. (1), the model parameters β, H, A_{sc}, C_p, ρ, L and c_f are, respectively, the irradiance efficiency and conversion factor related to the dimension of the collectors [m], global heat losses coefficient [W/^{o}C] per equivalent L tube length, pipe cross-section area [m^2], specific heat capacity of the water [J/kg^{o}C], water density [kg/m^3], equivalent absorber tube length [m], and the conversion factor from hours to seconds and for the equivalent collector tube length [s/h]. The parameter values and their further description are detailed in Pataro et al. (2022).

The FOPID is developed based on the linearized model of Eq. (1) in a specific approximated quasi-stationary point (considering a clear day with slight irradiance variations). Then, the inputs and the output values are obtained in this specific condition, defined as $\overline{T}_a$, $\overline{T}_{sc,in}$, $\overline{q}$ and $\overline{I}$ and $\overline{T}_{sc,o}$, respectively. Therefore, by employing the Taylor series expansions truncated in the first derivative and assuming the deviation variable notation $\check{\mathbb{X}}(t) = \overline{\mathbb{X}} - \mathbb{X}(t)$, the SCF linear model in Laplace frequency domain s is expressed as

$$\check{T}_{sc,o}(s) = \frac{K_I \check{I}(s) + K_{T_a} \check{T}_a(s) + K_{T_{in}} e^{-t_{d_{T_{in}}} s} \check{T}_{in}(s) + K_q e^{-t_{d_q} s} \check{q}(s)}{(\tau s + 1)} \tag{2}$$

where the model parameters are defined as

$$\begin{aligned} K_q &= \frac{-\frac{C_p \rho}{c_f L}(\overline{T}_{sc,o} - \overline{T}_{sc,i})}{\left[\frac{\rho C_p \overline{q}}{c_f L} + \frac{H}{2L}\right]} \qquad K_I = \frac{\beta}{\left[\frac{\rho C_p \overline{q}}{c_f L} + \frac{H}{2L}\right]} \\ K_{T_{sc,in}} &= \frac{\left[\frac{\rho C_p \overline{q}}{c_f L} - \frac{H}{2L}\right]}{\left[\frac{\rho C_p \overline{q}}{c_f L} + \frac{H}{2L}\right]} \qquad K_{T_a} = \frac{\frac{H}{L}}{\left[\frac{\rho C_p \overline{q}}{c_f L} + \frac{H}{2L}\right]} \\ \tau &= \frac{\rho C_p A_{sc}}{\left[\frac{\rho C_p \overline{q}}{c_f L} + \frac{H}{2L}\right]} \end{aligned} \tag{3}$$

As can be seen, the proposed linear model can change depending on the system conditions. Hence, the design of the feedback FOPID controller depends on the varying parameters $\tau(\overline{q})$ and $K_q(\overline{\Phi})$, for $\overline{\Phi} = [\overline{q}, \overline{T}_{sc,o}, \overline{T}_{sc,in}]$. Considering the actual operating limits of the CIESOL plant in a standard scenario, the water flow can vary from 3 m^3/h to 12 m^3/h and a $\Delta T = \overline{T}_{sc,o} - \overline{T}_{sc,in}$ from 3 °C to 10 °C. This operating range can cause the time constant to vary from $\tau_{min} = 17.53$ s to $\tau_{max} = 33.63$ s (91 %), the model gains K$_q$ from $K_{q_{max}} = -0.479$ (°C·h)/m^3 to $K_{q_{min}} = -1.84$ (°C·h)/m^3 (283 %) and the time delay from $d_{q_{min}} = 33$ s to $d_{q_{max}} = 53$ s (60 %) [1].

As seen, the parameters of the linear model undergo significant variations (as demonstrated through the percentage index relating the maximum and minimum constant values). Therefore, this study proposes two control architectures: first, an optimal-tuned FOPID controller focuses solely on the linearized model and its parameter uncertainties, excluding the varying time delays. This approach ensures robustness specifically to address the system's nonlinear aspects. Second, the challenge of varying time delays is managed by the nonlinear FSP structure. This

[1] The delay values are obtained from empirical validation experiments in the existing CIESOL facility.

decoupled control structure, FOPID + nonlinear FSP, enables a faster response in the closed-loop system while simultaneously handling the delay variations through the robust filter of the Smith predictor dead-time compensator.

3. FRACTIONAL ORDER PID DESIGN

The basis of FOPID controllers is to formulate the integral and derivative in terms of fractional calculus, which extends the order from integer to any real number. In this work, the Grümwald-Letnikov operator ${}_0\mathbf{D}_t^{\alpha}$ is applied to perform the integrals and derivatives in the form of

$$ {}_0\mathbf{D}_t^{\alpha} = \frac{d^{\alpha} f(t)}{dt^{\alpha}} = \lim_{h \to 0} \frac{1}{h^{\alpha}} \sum_{r=0}^{\frac{t-\alpha}{h}} (-1)^r \binom{n}{r} f(t - rh), \tag{4} $$

in which $\frac{t-\alpha}{h}$ is the integer part and α and t are the limits of the operator. Note that n is the integer value that satisfies the $n-1 < \alpha < n$ condition. Assuming $\alpha > 0$, the operator represents fractional differential. Conversely, if $\alpha < 0$, the operator represents a fractional integral (see (Shah and Agashe, 2016) for further details). Hence, one can apply the Grümwald-Letnikov operator to the control law of the PID controller, resulting in

$$ u(t) = K_p \left(e(t) + \frac{1}{T_i} {}_0\mathbf{D}_t^{\lambda} e + T_{d0} \mathbf{D}_t^{\mu} e \right). \tag{5} $$

Hence, by employing the Laplace transform in Eq. (5), the FOPID controller can be obtained as

$$ C(s) = \frac{U(s)}{E(s)} = K_p \left(1 + \frac{1}{T_i s^{\lambda}} + T_d s^{\mu} \right), \tag{6} $$

in which λ is the fractional order of the integral action and μ is the fractional order of the derivative action. Based on the presented control law, the FOPID includes two more degrees of freedom (λ and μ), which can increase the range of feasible solutions to achieve the proposed control performance compared to a standard PID controller. This work employs an optimization method to tune the FOPID controller, namely, parameters K_p, T_i, T_d, λ, and μ, to achieve the required closed-loop and robustness performance for SCF systems, following the methodology used in the literature (Elmetennani et al., 2017; Meng et al., 2020; Beschi et al., 2016).

3.1 Optimization tuning procedure

First, to consider an implementable FOPID controller, following the steps presented by Beschi et al. (2016), a fractional filter is included in the derivative term, resulting in the following solution

$$ C(s) = \frac{U(s)}{E(s)} = K_p \left(1 + \frac{1}{T_i s^{\lambda}} + \frac{T_d s^{\mu}}{\frac{T_d}{N^{\mu}} s^{\mu} + 1} \right). \tag{7} $$

in which $\frac{1}{N}$ is the filter time constant. In this work, $N = 100$ is chosen to exclude it from the decision variables of the optimization problem, as noisy signals are observed in this process. As noted in the results section, this solution is very promising for the SCF control problem.

Secondly, the optimization problem considers the entire range of possible combinations of τ and K_q. Note that the delay d_q is not considered in this stage since the nonlinear FSP framework will be imposed afterward. Hence, the process model is also dependent on the linear parameters in the form of

$$ P(s, \Theta) = \frac{T_{sc,o}(s)}{q(s)} = \frac{K_q(\overline{\Phi})}{(\tau(\overline{q})s + 1)}, \tag{8} $$

in which $[K_q(\overline{\Phi}),\ \tau(\overline{q})] \in \Theta$, $\Theta \subseteq \mathbb{R}^2$, $\tau(\overline{q}) \in [\tau_{min}, \tau_{max}]$ and $K_q(\overline{\Phi}) \in [K_{q_{min}}, K_{q_{max}}]$.

Assuming $C(s)$ and $P(s, \Theta)$, and considering $s = jw$ and $L(jw, \Theta) = C(jw)P(jw, \Theta)$, the following optimization problem is imposed to minimize the maximum sensitivity gain

$$ M_s = \max_{w} |S(jw, \Theta)| = \left| \frac{1}{1 + L(jw, \Theta)} \right|, \tag{9} $$

in the form of

$$ \min_{C(jw)} M_s, \tag{10} $$

subject to:

$$ \begin{aligned}
&\text{i) } w_c = 1\ rad/s \text{ , (desired gain crossover frequency);} \\
&\text{ii) } \phi_m = 85^o \text{ , (desired phase margin range);} \\
&\text{iii) } \left| \frac{1}{1 + L(jw, \Theta)} \right| < 0.01 \text{ , } \forall w < 10^{-4} \text{ , (load disturbance rejection performance);} \\
&\text{vi) } |T(jw, \Theta)| = \left| \frac{L(jw, \Theta)}{1 + L(jw, \Theta)} \right| < 0.01 \text{ , } \forall w > 10^{1} \text{ , (noise rejection performance).} \\
&\text{v) } -13.6 < K_p < -0.136; \\
&\text{vi) } 3.6 < T_i < 67.26; \\
&\text{vii) } 0 < T_d < 17.53; \\
&\text{viii) } 0.4 < \lambda < 1.8; \\
&\text{ix) } 0.1 < \mu < 1.8 \\
&\text{x) } C(jw) = K_p \left(1 + \frac{1}{T_i (jw)^{\lambda}} + \frac{T_d (jw)^{\mu}}{\frac{T_d}{N^{\mu}} (jw)^{\mu} + 1} \right).
\end{aligned} \tag{11} $$

The optimization procedure considers important aspects:

- The frequency range employed varies from 10^{-5} rad/s and 10^{2} rad/s considering the time constant frequency $w_{\tau_{min}} = 0.358$ rad/s and all the optimization constraints range;
- The range of all possible models is reduced to the vertices of the polytope composed by the maximum and minimum time constants and gains, that is, $\Theta_1 = (\tau_{min}, K_{q_{min}})$, $\Theta_2 = (\tau_{max}, K_{q_{min}})$, $\Theta_3 = (\tau_{min}, K_{q_{max}})$, and $\Theta_4 = (\tau_{max}, K_{q_{max}})$. This procedure allows to bound the entire combination of models and reduce considerably the computational cost;
- The choice of the closed-loop and robust performances (constraints i to iv) are based on the insights of the SCF system and following adequate design for FOPID in the literature (Elmetennani et al., 2017; Meng et al., 2020; Beschi et al., 2016);
- The FOPID controller parameter limits (constraints v to ix) are defined based on tuning the initial PID controller using the IMC tuning (Åström and Hägglund, 1995) for a nominal plant (τ_{max} and $K_{q_{max}}$, worst case scenario), to establish bound for a stable controller. Moreover, the $\lambda > 0.4$ limit guarantees the elimination of steady-state error.

Finally, the optimization problem is solved in a bi-level approach. First, the global Genetic Algorithm (GA) solver from MATLAB obtains a global solution at an upper level,

aiming to find the minimum M_s. In addition, this solution is refined by applying a gradient local method, using *fmincon*, from MATLAB. The lower-level optimization is also formulated to find the minimum M_s, but in this case, the optimal parameters found by the GA are considered as the initial guess of the decision variables. The presented optimization problem is computed offline since the FOPID controller parameters are fixed, and thus, no struggle related to the computational burden is accounted for in the proposal.

The optimization parameters for both solvers are defined in Table 1.

Table 1. Optimization solver options

	Options
fmincon	Algorithm: active-set Constraint Tolerance: 10^{-5} Step Size: $1.49 \cdot 10^{-8}$ Function Tolerance: 10^{-6} Max Evaluations: 10^5 Max Iterations: 400 Optimality Tolerance: $5 \cdot 10^{-4}$ StepTolerance: 10^{-6}
GA algorithm	Constraint Tolerance: 10^{-5} Crossover Fraction: 0.0200 Fitness Limit: -Inf Function Tolerance: 10^{-6} Max Generations: 500 Max Time: Inf Mutation Function: Gaussian operator Population Size: 200

3.2 Optimization results

The proposed bi-level algorithm is performed identically to the presented FOPID controller and to the conventional PID, in which the optimization parameters are merely K_p, T_i, and T_d. Table 2 depicts the obtained results for both controllers. The FOPID controller's additional

Table 2. Optimization results for the FOPID and conventional PID controllers.

	FOPID	PID
M_s (GA) [dB]	0.1059	0.495
M_s (*fmincon*) [dB]	0.1048	0.495
K_p [C°h/m^3]	-9.096	-8.590
T_i [s]	6.374	7.288
T_d [s]	0.0	0.0
λ [-]	0.83	1
μ [-]	-	-

degrees of freedom allow for better controller performance adjustment, obtaining a smaller sensitivity gain M_s than the PID. One can note that the derivative gain does not improve the control response for both strategies, which corresponds to conventional tuning for the SCF systems (Camacho et al., 2012). To satisfy the proposed closed-loop response and robustness performance, the FOPID obtained a slightly higher proportional gain, which allows the controller to have a faster response and keep the closed-loop stability for all the bounded linear model uncertainties. The main difference is observed in integral order, resulting in the main factor responsible for reducing the sensitivity gain for the FOPID controller.

Fig. 1 depicts the Bode diagram obtained from the optimization method for the FOPID only. As can be seen, the FOPID can address the robustness stability criteria defined in the optimization problem, obtaining a smaller sensitivity gain compared to the PID strategy.

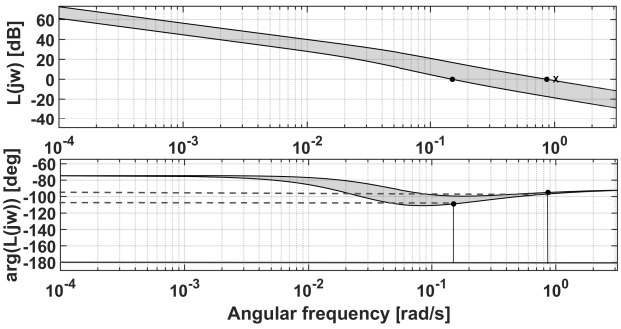

Fig. 1. Bode diagram for the FOPID optimal tuning parameters. The grey-shadow zone represents the combination of all possible models. The solid black lines are the bound formed by the vertices of the polytope of the $\tau(\overline{q})$ and $K_q(\overline{\Phi})$ extreme values. The "x" marks the gain crossover limit (constraint i of the optimization problem).

Furthermore, to demonstrate the effective solution of the optimization tuning regarding addressing all the model uncertainties using the polytope vertices, Fig. 2 depicts the reference tracking and disturbance rejection performance considering the entire range of $\tau(\overline{q})$, $K_q(\overline{\Phi})$, and for $K_{T_{sc,in}}(\overline{\Phi})$ [2]. This result is obtained assuming small gradients for each parameter and solving the closed-loop response for the combined solutions. For instance, $\tau(\overline{q}_1) = \tau_{min} + \delta\tau$, for $\delta\tau = 0.1$, from τ_{min} to τ_{max}, and so on for $K_q(\overline{\Phi})$ and $K_{T_{sc,in}}(\overline{\Phi})$ considering $\Delta T = \Delta T_{min} + \delta\Delta T$, with $\delta\Delta T = 0.1$. Although the optimization problem is formulated only considering the vertices of the polytope, the obtained tuning guarantees that all the linear model parameter uncertainties are accounted for, resulting in a robust solution for all possible model parameters. The result is also confronted by applying the constraint evaluation function for all possible models, which resulted in true outputs for all simulation experiments.

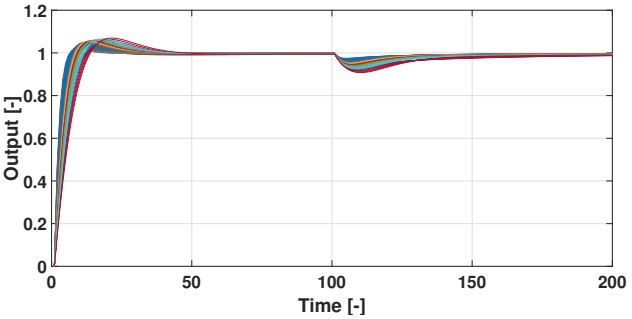

Fig. 2. Closed-loop response of the FOPID controller for all possible combinations of linear model parameters uncertainties.

[2] The simulation is presented only to demonstrate that the polytope vertices solution is effective to deal with all model combinations for the different parameters values. Hence, the inlet temperature was used as it obtained the higher gain among all disturbances.

Finally, considering a practical implementation of the obtained FOPID, a discrete approximation is obtained from the continuous transfer function of Eq. (7). The approximation is performed considering the Oustaloup filter (Oustaloup et al., 2000), using a zero-pole order of 3 and a frequency range from 10^{-4} rad/s to 10 rad/s. The results are confronted with the continuous transfer function obtained from the MATLAB toolbox FOMCON (Tepljakov et al., 2011). Figure 3 demonstrates that the approximated lead-lag discrete FOPID controller can respond similarly to the continuous solutions, obtaining slight differences for higher frequencies. Moreover, the response in the frequency domain approximates an integer order low-pass filter response due to the presented tuning detailed in Table 2. The FOPID response, although similar to integer order controllers, presents better robustness performance when comparing the Ms parameter in Table 2.

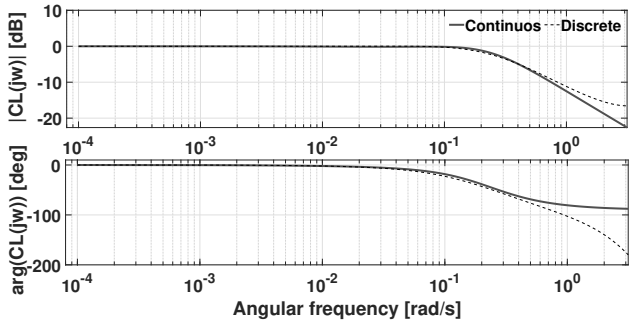

Fig. 3. Bode diagram comparison of the discrete approximation and continuous transfer function of the FOPID controller.

4. FOPID + NONLINEAR FSP IMPLEMENTATION

The presented FOPID controller is implemented with the nonlinear FSP to decouple the linear model uncertainties and the varying time-delay issues. The control scheme is formulated over the already developed lower-layer control, in which a PI with an Anti-Wind-up (PI-AW) scheme controls the pump velocity to achieve the desired water flow rate. Fig 4 details the complete control structure for the SCF in the CIESOL facility, in which 1 s sample time is applied to perform all computations required for the strategies. One can note that the chosen sample time is adequate considering the inner loop time constant (5 s) and outer loop fastest time constant (17.53 s), respecting a good trade-off for the ratio τ/T_s between 4 to 20 recommended in the literature. It must be noted that the lower-layer PI-AW presents a closed-loop time constant of 5 s, which is considerably faster than the SCF time constant, thereby being negligenced from the nonlinear model of the FSP compensator. The nonlinear model used for the FSP is defined in Eq. (1), using validated parameters to describe the SCF outlet temperature dynamics accurately. Although the filter F_r aims to achieve robustness regarding the varying time delay, this structure also improves robustness in closed-loop for model uncertainties, contributing to a steady behavior of the entire control architecture. Simulation tests were performed to tune the SP filter to achieve the desired behavior of the overall control structure. The delay model was considered 33 s (minimum delay found in the existing system). In contrast, the validated

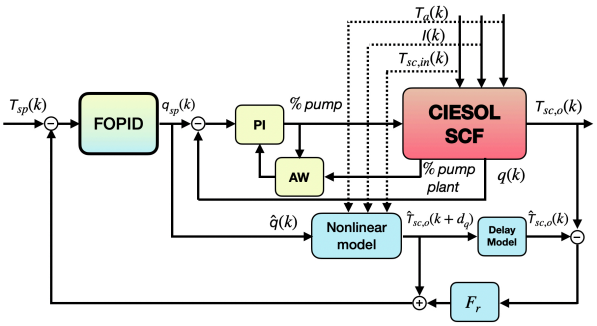

Fig. 4. General control scheme of the FOPID + nonlinear FSP for the SCF system of the CIESOL facility. The discrete-time delay approximation is defined as $d_q = t_{d_q}/Ts$.

model, representing the actual system, was assessed at 55 s (maximum delay found in the current system). The best trade-off in simulations was obtained with the tuning $F_r = 0.09516/(z - 0.9048)$ using the zero-order hold discretization transform and applying the proper design proposed in Normey-Rico and Camacho (2007).

Due to the length of the simulated analysis, only the implemented results of the FOPID + nonlinear FSP in the actual facility will be presented in this work. However, in simulations, the controllers are tested in a sunny day scenario, in which the FOPID obtained a sum of absolute error 3192.4 and a sum of the control increments 218.4, while the PID obtained 3188.6 and 332.5. As expected, these results represent a more conservative tuning of the FOPID with less aggressive movements of the control actions, characterizing a more robust behavior (see parameter Ms Table 2). Figure 5 displays the control of the SCF outlet temperature using the FOPID + nonlinear FSP in the actual CIESOL facility on October 13, 2023. It can be noted that the proposed FOPID obtained a fast response, with time constants of approximately 54 s average for the reference change scenario. Moreover, during the experiment, the irradiance variable was affected by high-frequency variations due to passing clouds. Correspondingly, the proposed FOPID could keep robust stability in a wide range of SCF operating conditions regardless of the disturbances while keeping an acceptable reference tracking performance. Notably, the implemented nonlinear FSP can adequately deal with variations of time delays as the water flow varies considerably during the trial, from its minimum to its maximum value. As a result, the overall control structure, FOPID + FSP plus the inner loop control PI-AW, presented a promising approach to control the SCF system, assuming robust behavior concerning multiple model uncertainties, dealing with model disturbances, and presenting satisfactory reference tracking for the wide range of the plant operation.

5. CONCLUSION

This study has introduced a novel approach to the control SCF, applying a robust-tuned FOPID associated with an FSP compensator structure. Two critical enhancements were presented in this research. First, the FOPID tuning method outperformed the conventional PID under the same optimization procedure. Secondly, combining a single FOPID controller and a nonlinear FSP compensator

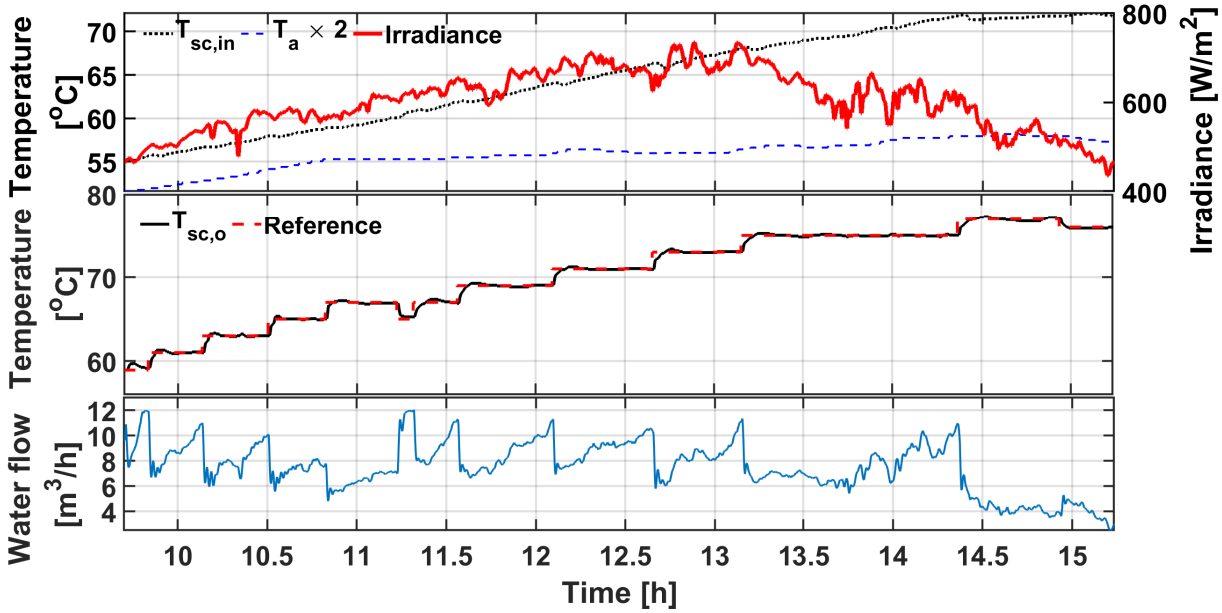

Fig. 5. Empirical results of the FOPID controller in the CIESOL facility.

bolstered the control structure by enabling the FOPID to deal with linear model uncertainties through robust design across the entire operating range. In contrast, the FSP compensator adeptly managed the variable time delays. Extensive control performance analysis was conducted, and implementing the FOPID strategy within the CIESOL facility demonstrated its remarkable effectiveness.

Future works intend to address and compare different tuning methods of FOPID for SCF systems. Moreover, further research aims to design a FOPID tuned with a linear FSP capable of optimally tuning the dead-time compensator with different tunings, such as lead filter with and without fractional order.

REFERENCES

Alilou, M., Azami, H., Oshnoei, A., Mohammadi-Ivatloo, B., and Teodorescu, R. (2023). Fractional-order control techniques for renewable energy and energy-storage-integrated power systems: A review. *Fractal and Fractional*, 7(5). doi:10.3390/fractalfract7050391.

Åström, K.J. and Hägglund, T. (1995). *PID controllers: theory, design, and tuning*. ISA-The Instrumentation, Systems and Automation Society.

Beschi, M., Padula, F., and Visioli, A. (2016). Fractional robust PID control of a solar furnace. *Control Engineering Practice*, 56, 190–199. doi:10.1016/j.conengprac.2016.04.005.

Camacho, E.F., Berenguel, M., Rubio, F.R., and Martínez, D. (2012). *Control of Solar Energy Systems*. Springer, London, England. doi:10.1007/978-0-85729-916-1.

Elmetennani, S., N'Doye, I., Salama, K.N., and Laleg-Kirati, T.M. (2017). Performance analysis of fractional-order PID controller for a parabolic distributed solar collector. In *2017 IEEE AFRICON*, 440–445. doi:10.1109/AFRCON.2017.8095522.

Meng, F., Liu, S., Pang, A., and Liu, K. (2020). Fractional order PID parameter tuning for solar collector system based on frequency domain analysis. *IEEE Access*, 8, 148980–148988. doi:10.1109/ACCESS.2020.3016063.

Normey-Rico, J.E. and Camacho, E.F. (2007). *Control of Dead-time Processes*. Springer, London, England. doi:https://doi.org/10.1007/978-1-84628-829-6.

Normey-Rico, J.E., Bordons, C., Berenguel, M., and Camacho, E.F. (1998). A robust adaptive dead-time compensator with application to a solar collector field. *IFAC Proceedings Volumes*, 31(19), 93–98. doi:10.1016/S1474-6670(17)41134-7. IFAC Workshop on Linear Time Delay Systems (LTDS '98), Grenoble, France, 6-7 July.

Oustaloup, A., Levron, F., Mathieu, B., and Nanot, F. (2000). Frequency-band complex noninteger differentiator: characterization and synthesis. *IEEE Transactions on Circuits and Systems I: Fundamental Theory and Applications*, 47(1), 25–39. doi:10.1109/81.817385.

Pataro, I.M.L., Gil, J.D., Americano da Costa, M.V., Guzmán, J.L., and Berenguel, M. (2022). A stabilizing predictive controller with implicit feedforward compensation for stable and time-delayed systems. *Journal of Process Control*, 115, 12–26. doi:10.1016/j.jprocont.2022.04.017.

Podlubny, I. (1994). Fractional-order systems and fractional-order controllers. *Institute of Experimental Physics, Slovak Academy of Sciences, Kosice*, 12(3), 1–18.

Shah, P. and Agashe, S. (2016). Review of fractional PID controller. *Mechatronics*, 38, 29–41. doi:doi.org/10.1016/j.mechatronics.2016.06.005.

Singh, S., Tayal, V.K., Singh, H.P., and Yadav, V.K. (2020). Fractional control design of renewable energy systems. In *2020 8th International Conference on Reliability, Infocom Technologies and Optimization (Trends and Future Directions) (ICRITO)*, 1246–1251. doi:10.1109/ICRITO48877.2020.9197902.

Tepljakov, A., Petlenkov, E., and Belikov, J. (2011). FOMCON: Fractional-order modeling and control toolbox for MATLAB. In *Proceedings of the 18th International Conference Mixed Design of Integrated Circuits and Systems - MIXDES 2011*, 684–689.